Cationic Phenoxyimine Complexes of Yttrium: Synthesis, Characterization, and Living Polymerization of Isoprene

Alexis Oswald, Ludmilla Verrieux, Pierre-Alain Breuil, Hélène Olivier-Bourbigou, Julien Thuilliez, Florent Vaultier, Mostafa Taoufik, Lionel Perrin, Christophe Boisson

Cationic Phenoxyimine Complexes of Yttrium: Synthesis, Characterization and Living Polymerization of Isoprene

Alexis D. Oswald,[a] Ludmilla Verrieux,[b,e] Pierre-Alain R. Breuil,[c] Hélène Olivier-Bourbigou,[c] Julien Thuilliez,[d] Florent Vaultier,[d,e] Mostafa Taoufik,[a,e,] Lionel Perrin[b,e,]* and Christophe Boisson[a,e,]**

[a] Univ de Lyon, Université Claude Bernard Lyon 1, CPE Lyon, CNRS, UMR 5128, Catalysis, Polymerization, Processes and Materials (CP2M), 43 Bd du 11 Novembre 1918, F-69616 Villeurbanne, France

[b] Univ de Lyon, Université Claude Bernard Lyon I, CNRS, INSA, CPE, UMR 5246, ICBMS, 1 rue Victor Grignard, F-69622 Villeurbanne cedex, France

[c] IFP Energies nouvelles, Rond-point de l'échangeur de Solaize, BP 3, 69360 Solaize, France

[d] Manufacture Michelin, 23 place Carmes Déchaux, F-63000 Clermont-Ferrand, France

[e] ChemistLab, Michelin CP2M ICBMS joint Research Laboratory, F-69616 Villeurbanne, France

yttrium • cationic complexes • phenoxyimine • synthesis • characterization • isoprene • living polymerization • DFT

ABSTRACT The phenoxyimine cationic complex [$L^1Y(CH_2SiMe_2Ph)(THF)_3$][BArF] ($L^1$ = (3-^{t}Bu)-(O)-C_6H_3-CH=N-(2,6-^{i}Pr-C_6H_3)) was prepared starting from the homoleptic [$Y(CH_2SiMe_2Ph)_3(THF)_2$] yttrium complex and the phenoxyimine ligand HL^1 and the subsequent cationization by the anilinium borate salt. The resulting complex was characterized by different techniques such as elemental analysis, NMR (^{1}H, ^{13}C, ^{89}Y) and more specifically by the ^{1}H-coupled ^{89}Y INEPT. The reactivity of the cationic complex towards isoprene polymerization was evaluated in presence of trialkylaluminum. This catalyst enables the living *cis*-1,4 polymerization of isoprene selectively. The influence and the role played by alkylaluminum is discussed based on the screening of set of aluminum reagents. By means of a computational mechanistic investigation performed at the DFT level, a cationic complex that account for the *cis* / *trans* / 3,4 selectivities experimentally observed is identified. Additionally, the *in silico* speciation of complexes resulting from the precatalytic mixture revealed the formation of stable Y/Al heterobimetallic complexes. Finally, for comparison purposes, the cationic amidinate yttrium complex [$L^2Y(CH_2SiMe_2Ph)(THF)_3$][$B(C_6F_5)_4$] ($L^2$ = PhC(N-2,6-^{i}Pr$_2C_6H_3$)$_2$) was synthesized and evaluated towards isoprene polymerization under similar conditions. This complex turned out to be active and selective towards the formation of 3,4-units.

INTRODUCTION

Cis-1,4 polybutadiene and polyisoprene are major constituents of rubber tires. To enlarge and/or shift material properties, the design of new catalysts able to polymerize stereospecifically conjugated dienes is still a major field of research. Additionally, the design of catalysts can still offer access to new advanced materials via their ability to copolymerize olefins and / or enable further macromolecular engineering.[1] Among the family of catalysts developed for conjugated

dienes polymerization, rare-earth metal catalysts are attractive and have provided a large range of polymer microstructures and in particular *cis*-1,4 polydienes.[2,3,4,5,6] More specifically, multicomponent catalysts have been developed industrially to produce butadiene rubber with very high *cis*-1,4 contents. These catalysts are generally based on a soluble rare-earth salt combined with an alkylaluminum and a halogenating agent such as alkylaluminum halides.[7,8] Though highly efficient, the structure of the catalytically active species of these catalytic systems remains unknown. Conversely, structurally well-defined and characterized alkyl and allyl rare-earth metal precursors are often used as model catalytic systems for the polymerization of conjugated dienes.[9,10,11,12,13,14] More recently a range of mono-ligated rare-earth metal complexes have been synthesized. They have been combined with a borane and borate salts to yield cationic active species. The control of the metal environment by the ligand enabled the control of the polydiene microstructures, offering access to well-defined polyisoprene with *trans*-1,4,[15,16] 3,4-[17,18,19,20] and *cis*-1,4-units[21,22,23,24,25,26,27,28] selectivities.

As an example of stereospecific polymerization of conjugated dienes, bis(phosphinophenyl)amido rare-earth metal catalysts yielded polyisoprene and polybutadiene with extremely high *cis*-1,4-selectivity under living conditions.[21] Most of these mono-ligated catalysts are based on dialkyl precursors in combination with a salt as activator based on anilinium or trityl tetrapentafluorophenylborate $[B(C_6F_5)_4]^-$ noted hereafter $[BArF]^-$. For these catalytic systems, the exact nature of the active species is questionable as the cationization for the synthesis of isolable cationic complexes or for polymerization initiation are not performed under the same conditions. Indeed, many cationic complexes have been isolated using $[BPh_4]^-$ as a counter-ion since it favors crystal formation and subsequent characterization by X-ray diffraction. However, to the best of our knowledge, none of these species are active toward isoprene polymerization.[29]

Within the few examples of cationic species implemented in isoprene polymerization the counter-anion is $[BArF]^-$. Among these examples, Okuda and coll. have isolated a cationic monocyclopentadienyl allyl yttrium complex that enables the polymerization of butadiene in the presence of triisobutylaluminum (TiBA),[10] and Hou and coll. have synthesized a THF free cationic monocyclopentadienyl allyl complex which polymerizes isoprene in absence alkylaluminum.[30]

In the process of designing high performance catalysts for both olefin polymerization[31,32] and ethylene trimerization,[33] phenoxy-imine proved to be a relevant ligand template. Although, Piers and coll. have isolated phenoxy-imine rare-earth complexes,[34] they have not been evaluated as polymerization catalysts. In the present communication, we report the synthesis of a cationic phenoxyimine yttrium complex that performs *cis*-1,4-selective isoprene polymerization using triisobutylaluminum as a cocatalyst. The activity and the stereospecificity of this catalyst have been compared to those of a cationic amidinate complex and of two homoleptic cationic complexes. The experimental investigation is amended by a computational mechanistic investigation performed at the DFT level to identify the dormant and active species involved in the selective catalytic polymerization process.

RESULTS AND DISCUSSION

Experimental Investigation

Synthesis of a cationic phenoxyimine yttrium complex. The synthesis of the mono-phenoxy-imine rare earth metal dialkyl complex $[L^1Y(CH_2SiMe_2Ph)_2(THF)]$ (**1**, L^1 = (3-^{t}Bu)-(O)-C_6H_3-CH=N-(2,6-^{i}Pr-C_6H_3), Scheme 1) was performed by protonolysis by the neutral ligand L^1H of the homoleptic trialkyl yttrium complex $[Y(CH_2SiMe_2Ph)_3(THF)_2]$ initially reported by Piers.[34] Complex **1** is stable up to 60 °C in THF solution. As discussed in our previous communication,[35] this stability seems to be brought by both the coordinated THF molecule, and the steric hindrance

and weak cation-π interactions originating from the Ph group of the alkyl ligand. These phenyl groups also play an additional role in controlling the stoichiometry of ligand exchange. Indeed, attempts of synthesizing a mono-phenoxyimine yttrium complex starting from the homoleptic trisneosilyl yttrium complex [$Y(CH_2SiMe_3)_3(THF)_2$] yielded a bis-phenoxyimine neosilyl complex. This point has been investigated computationally. Though ligands displacement by protonolysis is computed highly exergonic (ca. 50 kcal mol^{-1}), most likely due to the poor representation of solvation of the phenol function, single ligand exchange is computed more favorable by ca 10 kcal mol^{-1} between L^1H and [$Y(CH_2SiMe_3)_3(THF)_2$] than between L^1H and [$Y(CH_2SiMe_2Ph)_3(THF)_2$]. To a lesser extent, the second ligand exchange is computed more favorable by ca 6 kcal mol^{-1} for [$L^1Y(CH_2SiMe_3)_2(THF)$] than for [$L^1Y(CH_2SiMe_2Ph)_2(THF)$] to yield respectively [$L^1{}_2Y(CH_2SiMe_3)$] and [$L^1{}_2Y(CH_2SiMe_2Ph)$]. These calculations support the experimental trend and suggest that the mono-substituted yttrium complex can be more easily kinetically trapped using [$Y(CH_2SiMe_2Ph)_3(THF)_2$] than using its trisneosilyl analogue.

In terms of characterization, complex **1** was analyzed by ^{89}Y Insensitive Nuclei Enhanced by Polarization Transfer (INEPT) NMR experiment that has shown to reduce the acquisition time from 24 h to 30 min.[35] At 333 K, a good resolution of the spectrum was obtained for **1** (Figure S1). At this temperature, in THF-d_8, the Y chemical shift of **1** has been measured at 626.7 ppm, and the signal at 364.1 ppm was attributed to a small fraction of the bis-phenoxyimine complex [$L^1{}_2Y(CH_2SiMe_2Ph)$]. The 2D ^1H-^{89}Y NMR analysis of complex **1** highlights the coupling of yttrium with the imine proton (-CH=N) and with the two methylene carbons of the alkyl ligands (Figure S2). Under the reaction conditions used, mostly one alkyl group is exchanged via protonolysis with the phenoxyimine ligand. Starting from the complex **1**, the cationic complex

[$L^1Y(CH_2SiMe_2Ph)(THF)_3$][BArF] **1'** was prepared by reaction with the cationizing agent [PhNHMe_2][BArF] in THF (Scheme 1).

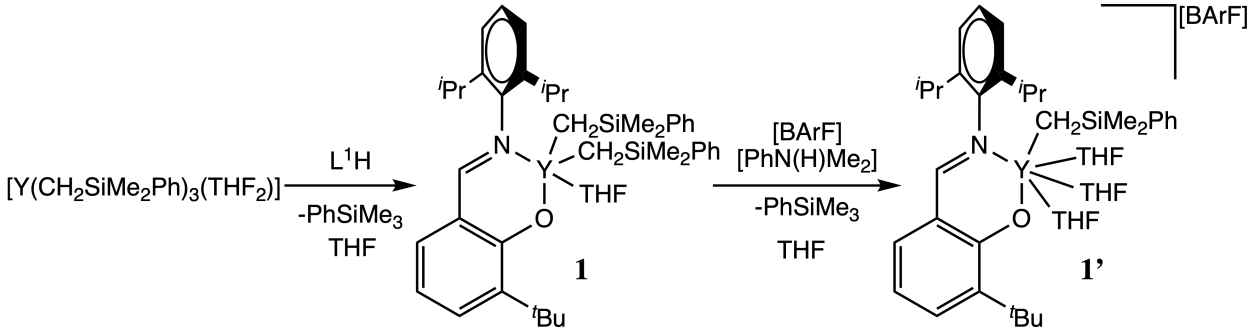

Scheme 1 Synthesis of the cationic mono-phenoxyimine mono-alkyl complex of yttrium **1'**.

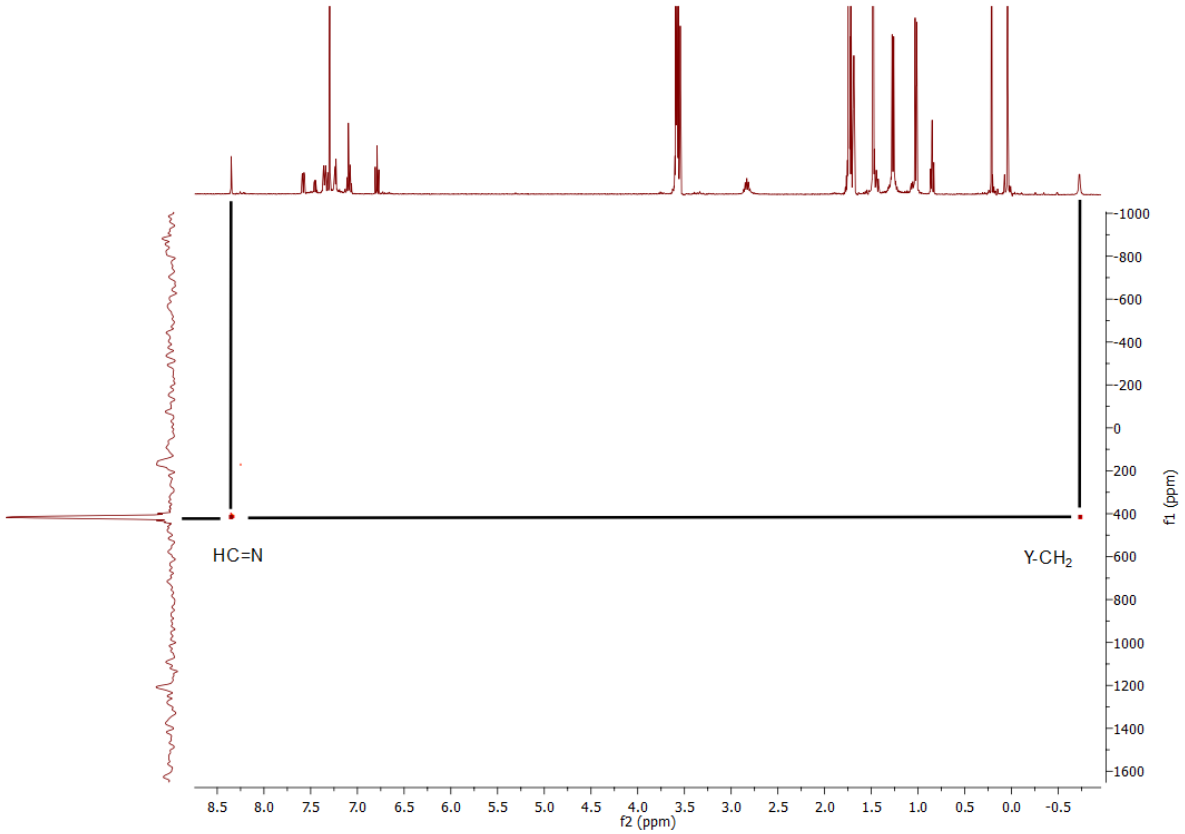

Figure 1 2D ^1H-^{89}Y NMR of cationic complex [$L^1Y(CH_2SiMe_2Ph)(THF)_3$][BArF] **1'** at 333 K in THF-d_8.

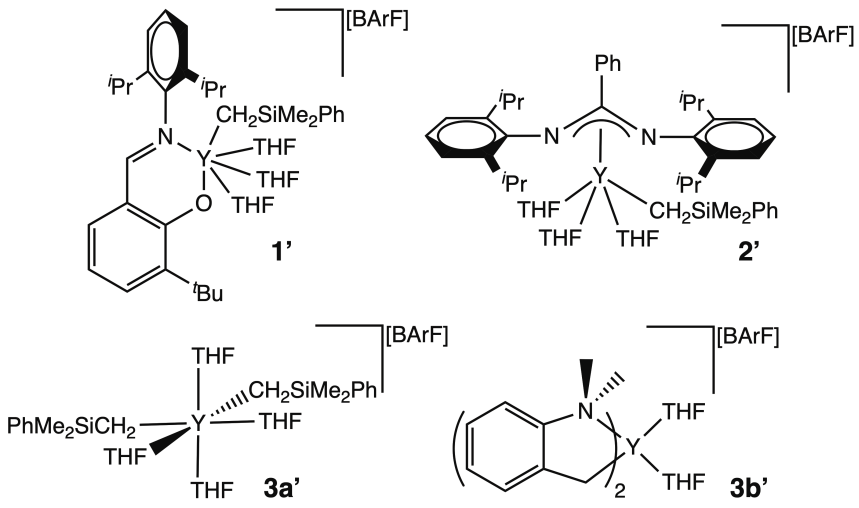

Scheme 2 Cationic complexes evaluated for isoprene polymerization.

The resulting cationic species was characterized by ^{1}H, ^{13}C, ^{19}F, ^{11}B, ^{89}Y NMR and elemental analysis as described in the experimental part. Upon cationization, the signal of yttrium is shifted up-field to 413.2 ppm. As for the neutral complex **1**, the 2D ^{1}H-^{89}Y NMR analysis of complex **1'** shows the coupling of yttrium with the imine proton (-C*H*=N) and with the methylene of the alkyl ligand (Figure 1). This agrees with the synthesis and the isolation of the alkyl mono-phenoxyimine cationic complex as depicted in Scheme 1. To the best of our knowledge, this is the first example of synthesis and isolation of a cationic mono-phenoxyimine complex of a rare earth element.

Synthesis of cationic amidinate yttrium complexes. As mono-amidinate rare earth complexes are reported as excellent catalysts for both ethylene[36,37] and isoprene[18,38] polymerizations, a mono-amidinate cationic yttrium complex was designed and prepared for comparison towards isoprene polymerization. Some mono-amidinate rare-earth metal cationic complexes were isolated by Hessen and coworkers.[36] These reported complexes displayed $[BPh_4]^-$ as a counter anion and were not evaluated in polymerization catalysis.

The synthesis of the precursor $[L^2Y(CH_2SiMe_2Ph)_2(THF)]$ (**2**) with L^2 = PhC(N-2,6-$^{i}Pr_2C_6H_3)_2$ of the mono-amidinate cationic yttrium complex was achieved using a procedure similar to that

reported in the literature for other amidinate complexes.[36] The cationic amidinate complex [L^2Y(CH_2SiMe_2Ph)($THF)_3$][BArF] **2'** (Scheme 2) was prepared via the cationization of complex **2** with [$PhNHMe_2$][BArF] in THF. Complex **2'** was fully characterized by NMR and elemental analysis. NMR of ^{89}Y showed a chemical shift at 526.0 ppm in THF-d_8 (Figure S13). In complex **2'**, three THF molecules are coordinated to the metal center as for the cationic complex **1'**.

Isoprene polymerization. We have previously reported that cationic bis(phenyldimethylsilylmethyl) (**3a'**) and bis(ortho-dimethylaminobenzyl) (**3b'**) complexes are active in the presence of triisobutylaluminum (TiBA) towards isoprene polymerization (Scheme 2).[35] They provide *cis*-1,4-polyisoprene with a low stereocontrol of 67 to 71%. These two cationic precursors provided similar polyisoprene microstructure (Table 1, runs 1 and 2)[35] which may suggest the formation of the same active species in the presence of TiBA under the polymerization conditions.

The efficiency of initiation is determined from the number of chains (n_{chains} = m(PI) / M_n) per yttrium. As previously reported by us,[35] a low efficiency is obtained for **3a'** presumably due to the presence of four molecules of THF. In both cases, a relatively high dispersity (1.57 and 1.64) is measured. This result has been ascribed to a slow initiation compared to propagation. These initial tests provide reference activities and selectivities relative to which phenoxyimine cationic based catalysts can be compared. In the absence of triisobutylaluminum (TiBA), the mono-phenoxyimine cationic complex [L^1Y(CH_2SiMe_2Ph)($THF)_3$][BArF] **1'** shows no activity towards isoprene polymerization (Table 1, run 3). Initiation of the polymerization reaction by the cationic complex requires the addition of at least 5 equivalents of TiBA relative to the yttrium cationic complex **1'** (Table 1, runs 4, 5). By increasing the [Al]/[Y] ratio up to 10 equivalents (Table 1, run 6), initiation efficiency raises up to ca. 100 %, i.e. one chain per yttrium is initiated.

Table 1 Isoprene polymerization assays.

run	complex/AlR_3 (T)[a]	[Al]/[Y]	time (min.)	conv. (%)	M_n[c] (Đ) (g mol^{-1})	chains/Y	3,4 / *cis*-1,4 / *trans*-1,4[d]
1	**3a'**/TiBA	10	60	92	477 000 (1.57)	0.38	25/71/4
2	**3b'**/TiBA	10	60	100	173 000 (1.64)	1.16	28/67/5
3	**1'**	-	60	0	-	-	-
4	**1'**/TiBA	3	60	traces	-	-	-
5	**1'**/TiBA	5	30	59	176 000 (1.01)	0.67	10/88/2
6	**1'**/TiBA	10	60	89	185 000 (1.03)	0.97	10/86/4
7	**1'**/TiBA	10	10	29	67 000 (1.12)	0.89	10/88/2
8	**1'**/TiBA	10	15	51	99 000 (1.02)	1.01	10/88/2
9	**1'**/TiBA	10	20	54	119 000 (1.13)	0.92	10/88/2
10	**1'**/TiBA	10	30	67	162 000 (1.02)	0.83	10/88/2
11	**1'**/TiBA (10°C)	10	60	21	72 000 (1.13)	0.55	10/89/1
12	**1'**/TiBA (20°C)	10	60	69	152 000 (1.02)	0.90	10/88/2
13	**1'**/TiBA (50°C)	10	60	100	207 000 (1.09)	0.97	10/83/7
14	**1'**/$Al(CH_2SiMe_3)_3$	10	60	0	-	-	-
15	**1'**/$Al(CH_2CMe_3)_3$	10	60	33	80 000 (1.05)	0.83	9/76/16
16	**1'**/$HAl(^iBu)_2$	10	60	79	30 000 (1.53)	5.25	10/86/4
17	**1'**/$Al(Oct)_3$	10	60	63	104 000 (1.18)	1.2	10/85/5
18	**1'**/TiBA	20	60	87	108 000 (1.19)	1.62	10/86/4
19	**1'**/TiBA	40	60	91	57 000 (1.23)	3.17	11/85/5
20[b]	**1**/TiBA	10	60	82	206 000 (1.09)	0.79	9/89/2
21[b]	**2**/TiBA	10	60	84	151 000 (1.19)	1.01	91/4/5
22	**2'**/TiBA	10	60	89	177 000 (1.07)	1.11	91/4/5

[a] General polymerization conditions: 40 mL toluene, 30 °C, n(complex) = 10 µmol, [isoprene]/[Y] = 3000; [b] Addition of $[CPh_3][B(C_6F_5)_4]$ after precontact of the complex with TiBA ([B] / [Y] = 1); [c] Determined by size exclusion chromatography with light scattering; [d] Determined from ^1H and ^{13}C NMR spectrum of polyisoprene.

The analysis by ^{1}H and ^{13}C NMR of the polymer microstructure reveals that a higher *cis*-1,4 contents (85-89%) is obtained when the metal is supported by a phenoxyimine ligand (Figures S16 and S17). Additionally, the presence of this ligand contributes to a better control of the molar mass distribution as indicated by a measured Đ of 1.03. Polymerization assays were performed at various length of time (Table 1, runs 6-10). As shown in Figure 2, a linear increase of molar masses is observed with increased conversion, while the dispersity remains low (Đ= 1.02-1.12). This pattern is characteristic of living polymerization. Polymerization assays were also performed at various temperature ranging from 10°C to 50°C (Table 1, runs 6 and 11-13). This set of experiments reveals the influence of the temperature on the initiation efficiency. At 10 °C the efficiency is only of 55 % but reaches 90 % at 20 °C. Additionally, a faster polymerization rate was observed at 50 °C without significant broadening of molar mass distribution. This highlights that the polymerization is still controlled at this temperature.

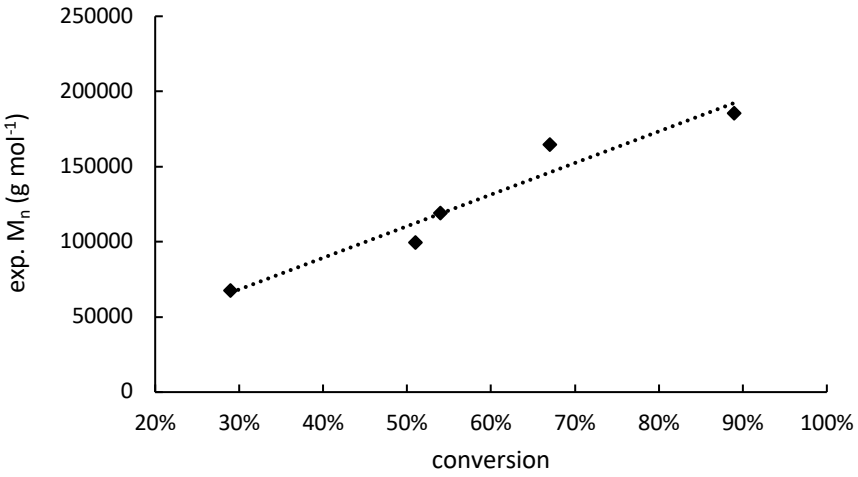

Figure 2 Number average molar mass vs conversion, and linear fit (M_n = 210389**conv* + 5163.4, r^2= 0.94), for the isoprene polymerization catalyzed by the catalytic system **1'** / TiBA ([Al] / [Y] =10) at various times 10, 15, 20, 30 and 60 minutes.

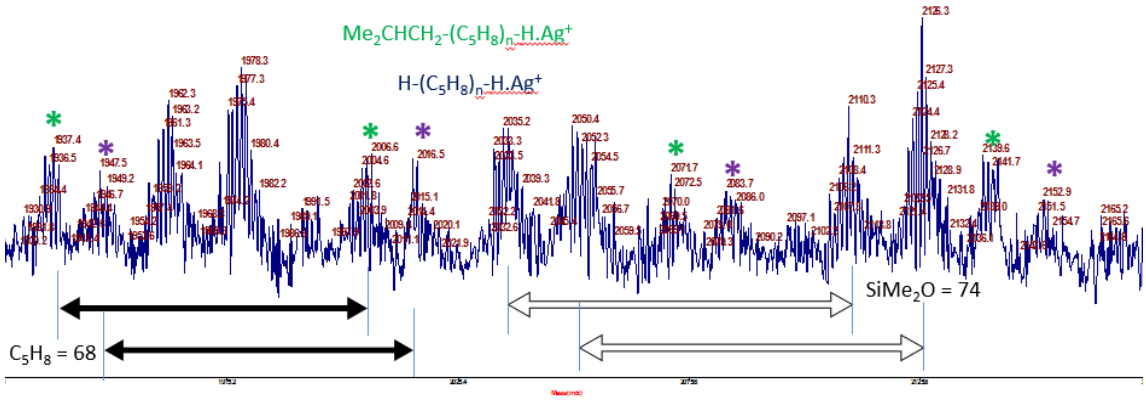

Figure 3 MALDI-TOF reflectron positive mode of IP catalyzed by **1'**/TiBA ([Al] / [Y] = 10).

The influence of the [Al] / [Y] ratio and the type of alkylaluminum have been varied to investigate the influence of the aluminum compound. First, the need of adding at least 5 equivalents of alkylaluminum to initiate polymerization highlights the role of THF scavengers. This is supported by the computed exergonicity of ca. 11 kcal mol^{-1} associated to the coordination of free THF to TiBA. Hence, the trapping of THF molecules coming from the yttrium precursor raises its electrophilicity and favors subsequent association with aluminum reagent and monomer as discussed below Scheme 5). A second role of TiBA could be to alkylate the metal center. This has been evidenced by analyzing polymer chain ends. Hence a MALDI-TOF mass spectrometry analysis was performed on a low molar mass polyisoprene synthesized by the catalytic system **1'** / TiBA. As shown in Figure 3, the mass spectrum displays two main isotopic distributions which corresponds to $[(CH_3)_2CH\text{-}CH_2\text{-}(C_5H_8)_n\text{-}H\bullet Ag]^+$ and $[H\text{-}(C_5H_8)_n\text{-}H]\bullet Ag^+$ The sample was unfortunately polluted by polydimethysilane due to the presence of grease. This result confirms the alkylation of the catalyst precursor with TiBA and that initiation takes place in the yttrium-isobutyl bond. The ability of aluminum-hydride to initiate the polymerization raised our attention especially regarding the purity of the trialkylaluminum used in polymerization assays. Indeed, the NMR analysis of several fresh batches of commercial TiBA showed the presence of about 10% of

$HAl(^{i}Bu)_2$. Hence, isoprene polymerization could be initiated by monomer insertion in the yttrium-hydride complex resulting from hydride transfer from aluminum to yttrium (Figure 3). The scope of tested aluminum derivatives was extended to diisobutylaluminum hydride as a cocatalyst (Table 1, run 16). In this case, a lower M_n of 30,000 g mol^{-1} and a broader molar mass distribution of 1.53 were obtained. With more than 5 chains per Y initiated, $HAl(^{i}Bu)_2$ appears as a better chain transfer agent than trialkylaluminium compounds. If the transmetalation between yttrium-polymer and aluminum-hydride bonds is considered, a transfer efficiency of 55% can be estimated. The catalyst **1'** / $HAl(^{i}Bu)_2$ thus displays a mechanism of coordinative chain transfer polymerization (CCTP) for isoprene polymerization.[39]

The MALDI-TOF mass spectrometry analysis suggests that $Y\text{-}CH_2SiMe_2Ph$ does not initiate isoprene polymerization. In agreement with this outcome, we showed that addition of 10 equivalents of trineosilylaluminum $Al(CH_2SiMe_3)_3$ on complex **1'** did not yield an active species (Table 1, run 14). Similarly, Carpentier and coll. have reported the absence of activity of a neosilyl *ansa*-yttrium complex towards styrene polymerization.[40] However, we can mention that the bisneosilyl bis(phosphinophenyl)amido yttrium complex polymerized isoprene in the absence of TiBA when activated with $[PhNHMe_2][B(C_6F_5)_4]$.[21] In order to discuss the steric or electronic origin of this lack of reactivity, the trineopentylaluminum and trioctylaluminum were also assessed as cocatalysts (Table 1, run 15 and 17). In both cases, good initiation efficiencies were observed. Isolated polyisoprene showed a narrow molar mass distribution of 1.05 and 1.18 respectively. As expected, the MALDI-TOF analysis highlighted the initiation of the polymerization by a neopentyl group (Figure S19 and S20). However, polymerization rates are slower than the one determined for TiBA, the lowest rate being measured for $Al(CH_2CMe_3)_3$. The stereospecificity of the

polymerization follows the same trend and suggests that a heterobimetallic compound is involved in the polymerization mechanism. This point is addressed in the computational section below.

The combination of **1'** with 10 equivalents of TiBA provided a living catalyst displaying one growing polymer chain per yttrium (Table 1, run 6). The addition of higher amount of TiBA (20 and 40 equivalents) (Table 1, runs 18 and 19) led to a decrease of molar masses at similar isoprene conversion together with a broadening of the molar mass distribution. This result is explained by chain transfer to aluminum,[41,42] though its efficiency is low ca. 9 % (see experimental part for details). The kinetic monitoring of the isoprene polymerization mediated by the **1'** / TiBA catalytic system showed a polymerization first order with respect to isoprene (Figure 4). For comparison, the neutral phenoxyimine complex **1** was activated with TiBA and trityl borate $[CPh_3][B(C_6F_5)_4]$ (Table 1, run 20). Even if a slightly better stereospecificity was observed, the initiation was less efficient, and dispersity was higher when using the neutral precursor. This set of experiments outlines that Y-based phenoxyimine catalysts are selective for *cis*-1,4 isoprene polymerization and that their cationic complexes can be used as precursor instead of neutral species activated *in situ*.

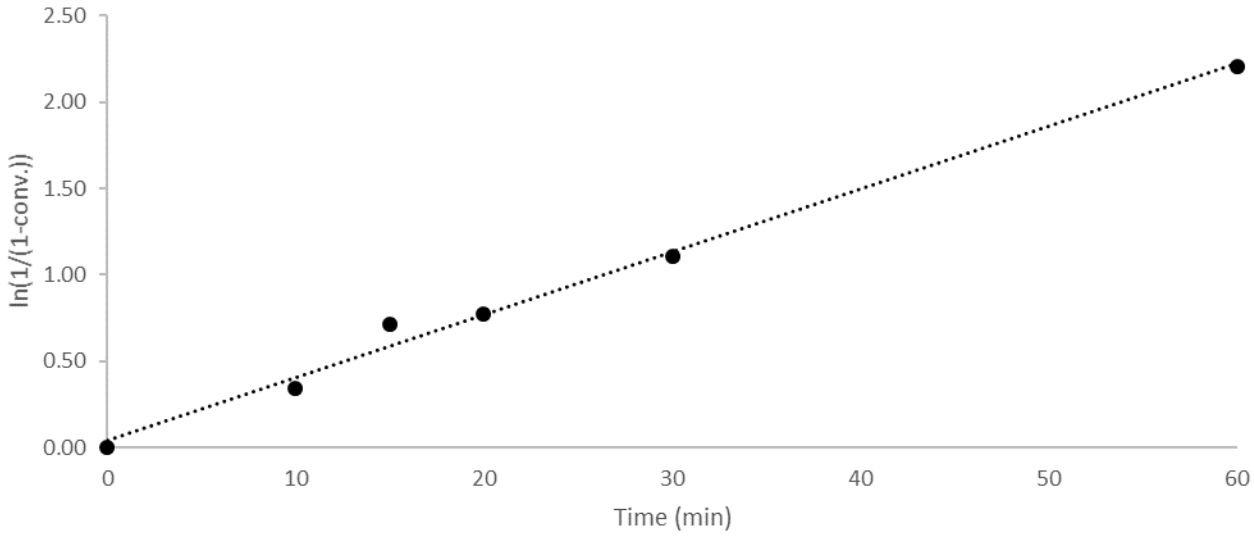

Figure 4 Plot of $\ln[(1\text{-conv.})^{-1}]$ (conv. is the conversion) vs time for isoprene polymerization catalyzed by **1'** / TiBA ([Al] / [Y] = 10) at various conversion 29, 51, 54, 67, and 89 %. Linear fit: $\ln[(1\text{-conv.})^{-1}] = 0.0364*t + 0.04$ ($r^2 = 0.992$).

To broaden the scope of this study and to explore the selectivity yielded by cationic yttrium-based complexes, the mono-amidinate neutral complex **2** and the resulting cationic complex **2'** were prepared. The synthesis of monoamidinate rare earth cationic complexes was previously reported by Hessen and coll.[36] using $[BPh_4]^-$ as a counter-anion but the complexes were not implemented in isoprene polymerization. Previously Hou and coll. showed that this class of catalyst led to 3,4-polyisoprene.[18] As expected, the activation of the neutral complex **2** with TiBA and $[CPh_3][B(C_6F_5)_4]$ ([Y] / [Al] / [B] = 1/10/1) provided a stereospecific 3,4 catalyst for isoprene polymerization (Table 1, run 21). The cationic catalyst **2'** / TiBA ([Al] / [Y] = 10, Table 1, run 22) displayed the same stereospecificity but with a better efficiency and narrower molar mass distribution (Đ= 1.07). Remarkably, the amidinate based catalyst **2'** / TiBA ([Al] / [Y] = 10) is *3,4*-stereospecific and enables a living polymerization.

Computational Mechanistic Investigation

The experimental study reported above has been complemented by a computational mechanistic investigation performed at the DFT level. This modeling section aims at identifying the catalytic active specificities that account for the selectivity observed experimentally. This computational study focuses only on mono-phenoxyimine cationic complex **1'**. To reduce the computational costs and additional sampling, the influence of the counterion has not been explicitly considered in the chemical model unless specified. Indeed, we have demonstrated in a previous study that the modeling of the counter-ion is needed to quantitatively estimate selectivities.[43]

Computational approach. Electronic structure calculations were performed at the DFT level using the B3PW91[44,45] hybrid functional and Gibbs energies were estimated at 298 K and 1 atm, and corrected by a D3-BJ single point dispersion correction.[46,47] Solvation was represented by a microsolvation approach using the SMD continuum model[48] in combination with some explicit coordinated solvent molecules. Geometries were fully optimized without constraint, connectivity of transition states were confirmed by IRC following. Conformational sampling was performed by hand, as exhaustively as possible. This modelling strategy proved to be robust in previous computational studies of similar polymerization catalytic systems.[35,43,49]

Notations. Insertion sequences are defined as follow. As the primary insertion of isoprene produces an alkyl site, the secondary insertion forms an allyl site, and due to the additional methyl group, four types of insertion can be defined as 1,2-primary (^{12}I), 4,3-primary (^{43}I), 2,1-secondary (^{21}I) and 3,4-secondary (^{34}I) (Scheme 3). In total, eight types of insertion can be defined with *cis* / *trans* isomerization of the monomer. Unless specified, the eight types of insertion defined above follow the same reactivity trends, independently of positioning of the Me group (Table S3 and S4). Thereof, for the sake of clarity and to simplify energy profiles, not all the possible pathways are presented and discussed. Additionally, in the metal-allyl group of $[M(\eta^3\text{-}RC_3H_3(Me))]^+$ (M = [L^1-Y]) insertion can either take place at the central M-C^3 bond of the allyl group leading to a ^{21}I unit or ^{34}I unit, or at the terminal M-C^1 bond of the allyl group yielding a ^{14}I unit or a ^{41}I unit. (Scheme 3) The *supine* / *prone* isomerism of the diene relative to ligand has also been considered and sampled. It is labelled *s* or *p* as defined in Scheme 4. Finally, transition states are noted with an asterisk (e.g. ^{14C}I^{12C}I*) and monomer adducts with an underscore (e.g. ^{14C}I_^{12C}I).

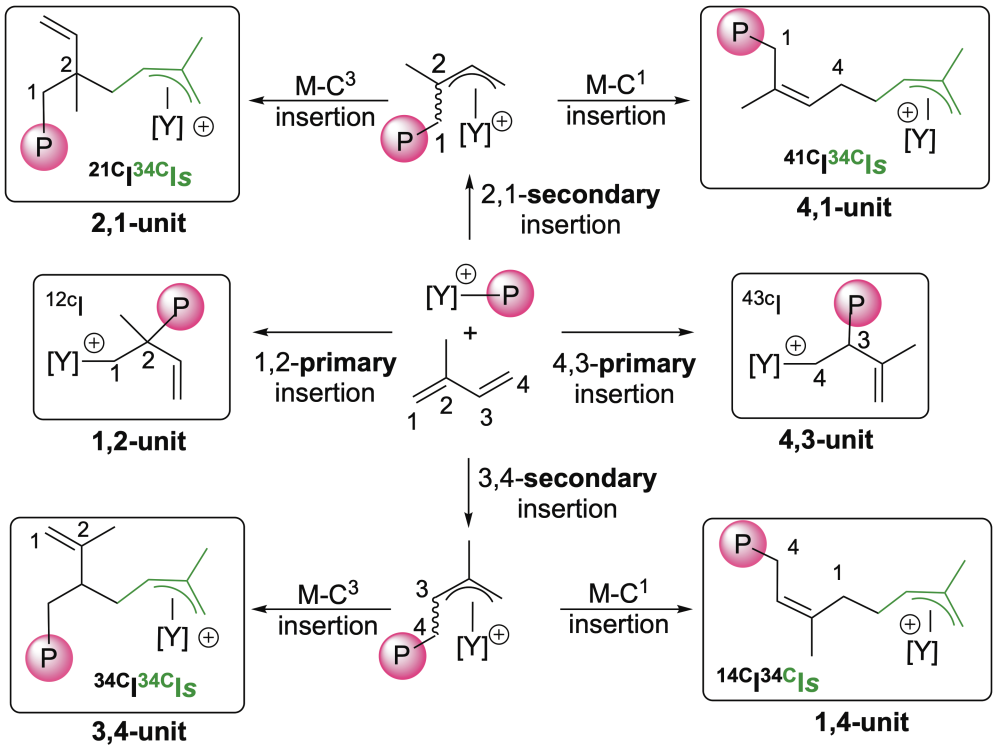

Scheme 3. Definition of unit formed after primary or secondary insertion at the central or terminal metal-allyl site and depending on the positioning of the methyl group. The name of the unit formed is in bold and an example of product geometry is given. The pink ball represents the polymer chain.

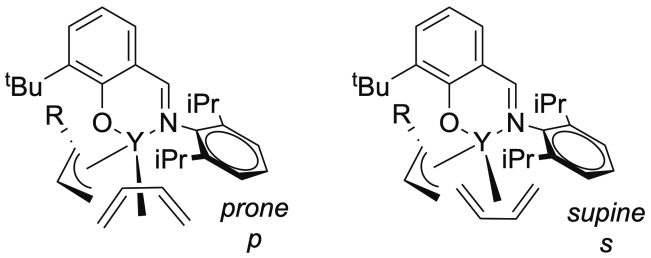

Scheme 4. Definition of *prone* and *supine* isomerism in the case of butadiene insertion, the polymer chain is noted R.

Speciation of Al, Y and Y/Al species. A speciation study has been initially performed to identify the most stable structure(s) of each species resulting from the association of the Y-based complex and the Al-based co-catalyst. The mono-phenoxyimine cationic complex

$[L^1Y(CH_2SiMe_2Ph)(THF)_3]^+$ **4** has been optimized in absence of the counter-ion. In the optimized structure, one of the three THF molecules is displaced in the second coordination sphere. The analogous complex $[L^1Y(CH_2SiMe_2Ph)(THF)_2]^+$ **5** solvated by only two THF molecules has been optimized. Relative to **4**, the formation of **5** is exergonic by 9.2 kcal mol^{-1}. Concerning the aluminum reagent, the isobutyl group of TiBA has been modelled in a first assumption by an ethyl group to avoid the extensive conformational sampling originating from the three ^{i}Bu groups. Concerning $AlEt_3$, the most stable structure is a dimer in which the double bridge displays a *trans*-periplanar configuration. Relative to separated $AlEt_3$, dimerization into Al_2Et_6 is exergonic by 10 kcal mol^{-1}. Finally, as the influence of the number of equivalents of trialkylaluminum on the activity has been evidenced experimentally, we have chosen a stoichiometry of 6 equivalents of trialkylaluminum per Y in the chemical model. Indeed, the highest conversion rates were obtained using 10 equivalents of TiBA with respect to Y, but if 3 equivalents are used, traces of polymerization are obtained, and with 5 equivalents the conversion rate is limited to 59%.

From the cationic species **5**, the formation of two bridged bimetallic complexes is computed thermodynamically favorable. In **6a**, the $-CH_2SiMe_2Ph$ group is bridging Y and Al while it occupies a terminal position at Al in **6b**. The driving force of this reaction is the coordination by aluminum of the THF molecules that are released by the Y complex **5**. The quenching of THF by the organoaluminum reagent is exergonic by 11.3 kcal mol^{-1} (Scheme 5). As the thermodynamics of formation of **6a** and **6b** only differ by 3 kcal mol^{-1} (Scheme 5), the $-CH_2SiMe_2Ph$ group does not strongly contribute to the stabilization of the Y cationic side of the complex though cation-π interaction. Consequently, due to the awaited exchange between **6a** and **6b**, the silyl group may not be initiating the polymerization. Based on this result, we have modelled the $-CH_2SiMe_2Ph$ group by an Et group for the investigation of the initiation mechanism of isoprene polymerization.

This simplification leads to the triply bridged cationic complex $[L^1Y\text{-}(\mu\text{-}Et)_3\text{-}AlEt]^+$ **6c** that is computed as the most stable isomer for this structure.

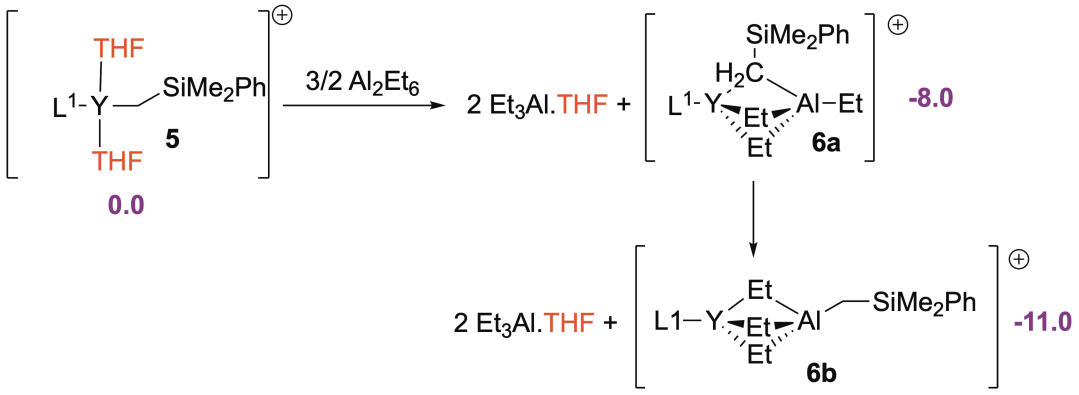

Scheme 5. Interaction between complex **6** and aluminum reagents. Relative Gibbs Energies in violet kcal mol^{-1}. The counter-anion is not included.

Reactivity study – polymerization initiation. To assess the active or dormant character of the bimetallic complex **6c**, optimization of transition states for monomer insertion in either Al-C terminal or bridged bonds and Y-C bridged bonds have been attempted. In this part, isoprene has been modeled by butadiene to restrict the sampling and to reduce the steric hindrance of the monomer. Optimized transition states either give activation energies that are above 35 kcal mol^{-1} and/or lead to the dissociation of the Y / Al dimer (see SI, Scheme S1 and Table S1). This supports the hypothesis that bimetallic species such as **6c** are dormant and lead us to the exploration of the reactivity of the cationic Y-based monometallic complexes. The dissociation of the Y / Al dimer **6c** into $[L^1\text{-}Y\text{-}Et]^+$ **7** and half equivalent of aluminum dimer are computed endergonic by 14.5 kcal mol^{-1} and is thus unlikely. However, energy barriers for the 3,4 insertions of isoprene into the Y-Et bond of $[L^1\text{-}Y\text{-}Et]^+$ are ranging from 4.0 to 4.4 kcal.mol^{-1} respectively for *cis*-3,4- and *trans*-3,4-insertion. This results in overall Gibbs energy barriers of ca 19 kcal mol^{-1} (see SI, Table S2), that are high but realistic relative to the polymerization conditions. Based on the approximations made on the chemical model, a Gibbs energy span of 2.0 kcal mol^{-1} between insertion transition

states can be interpreted as effective competitive pathways. Additionally, as the isoprene insertion is computed highly exergonic by ca. 12.5 kcal mol^{-1} relative to **6c** and as the Gibbs energy between the resulting *syn*- (**^{34T}I**) and *anti*-allyl complexes (**^{34C}I**) only defers by 0.8 kcal mol^{-1}, allyl isomerization will merely change the balanced proportion between these two complexes. Thereof, the first monomer insertion will preferentially yield the *syn*-allyl complex **^{34T}I** that will turn into a 1,4 isoprene unit upon second monomer insertion as discussed below.

Experimentally, as the nature of the aluminum reagent slightly influences the selectivity of the polymerization catalyst, the formation of dormant or active bimetallic allyl complexes has been considered computationally. Starting from the allyl complexes **^{34T}I** or **^{34C}I**, the association with half an equivalent of Al_2Et_6 is respectively exergonic by 5.7 and 11.9 kcal mol^{-1}. This sets the bimetallic complexes **^{34C}I•AlEt$_3$** as the most stable complex during the propagation (Figure 5). For both **^{34C}I•AlEt$_3$** and **^{34T}I•AlEt$_3$** bridging allyl / terminal alkyl exchange is computed endergonic 6.7 and 4.0 kcal mol^{-1} and the subsequent dissociation into $[L^1Y\text{-}Et]^+$ and half equivalent of $Et_4Al(allyl)_2$ is endergonic by at least 12.2 kcal mol^{-1}. This reaction pathway, that traduces chain shuttling and the potential initiation a second polymer is thermodynamically highly unfavorable. This is in line with the experimental determination, for this catalytic system, of a poorly efficient Y / Al chain shuttling and of one growing polymer chain per yttrium centre. For comparison, a similar trend were computed for the Nd / Mg catalytic system used in ethylene / butadiene copolymerization and for which alkyl groups can shuttle between Nd and Mg, but allyl groups resulting from butadiene insertion at Nd cannot be transferred to Mg.[50,51,49] However, for the Y / Al system bimetallic complexes that are bridged by an allyl and an alkyl groups (e.g. **^{34C}I•AlEt$_3$**) are thermodynamically more stable than the separated monometallic complexes, whereas the

formation of such complexes were computed thermoneutral or slightly endergonic for the Nd / Mg system.[51]

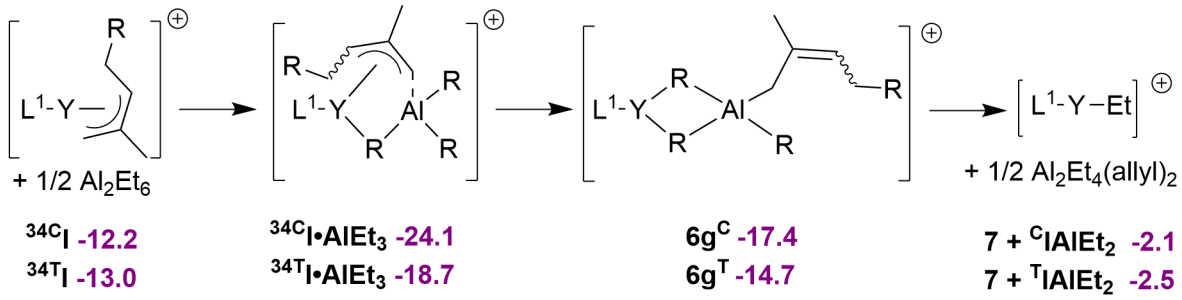

Figure 5. Computed Gibbs energies in kcal mol^{-1} for the formation of Y / Al bimetallic intermediates and subsequent allyl / alkyl exchange starting from yttrium allyl complexes and trialkylaluminum reagent. Energy reference is **6c** with *trans*-isoprene.

Reactivity study – selectivity of polymerization propagation. Transition states for isoprene insertion within the heterobimetallic allyl systems ^{34C}**I•AlEt$_3$** and ^{34T}**I•AlEt$_3$** have been first considered. Despite our efforts, all attempts did not reach full convergence and often led to the dissociation of the bimetallic complex. Thereof, we have optimized isoprene insertion transition state at monometallic allyl complexes ^{34C}**I** and ^{34T}**I**. Energy profiles for isoprene insertion in the Y-allyl site of both ^{34C}**I** and ^{34T}**I** are summarized in Figure 6.

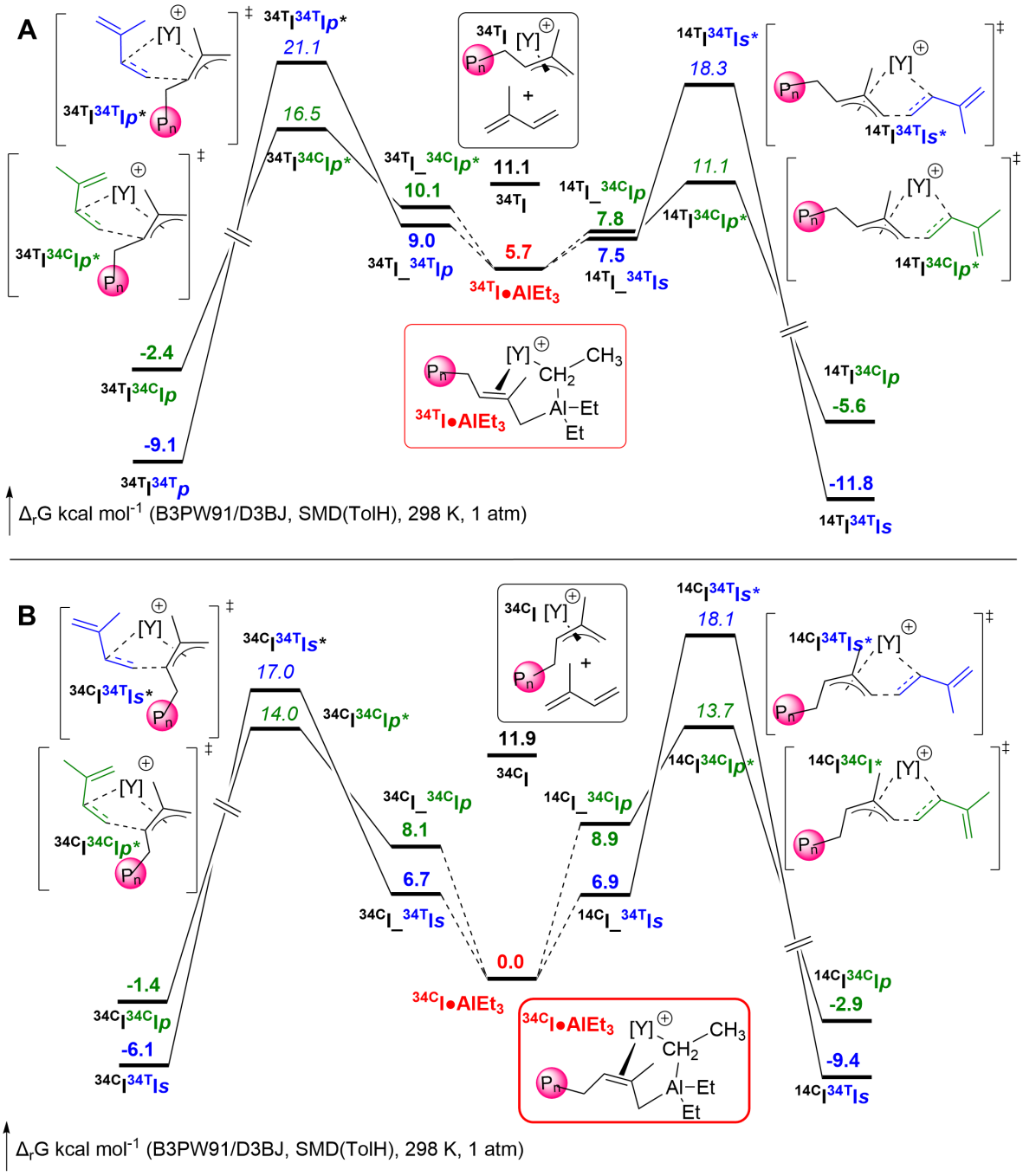

Figure 6 Gibbs energy profile of the propagation step for the isoprene homopolymerization ΔG (kcal mol^{-1}). P_n = Et. Energies referring to kinetics are in italic and energies referring to thermodynamics are in bold. Only the lowest energy barriers are presented, all explored possibilities / isomers are available in SI (Table S3 and S4). Energy reference is **^{34C}I•AlEt$_3$** and *trans*-isoprene.

For clarity, only the lowest energy pathways have been represented, alternative possibilities are available in the SI. Starting from *syn*-allyl active site ^{34T}**I•AlEt$_3$** (Figure 6.A), coordination of *trans*-isoprene to Y and release of half Al_2Et_6 is endergonic by 1.8 kcal mol^{-1} and favored over coordination *cis*-isoprene by less than a kcal mol^{-1}.

Reversely, insertion of *cis*-isoprene in either the terminal (transition state ^{14T}**I**^{34C}***Ip****) or central Y-allyl (transition state ^{34T}**I**^{34C}***Ip****) bond are kinetically favored over the *trans*- insertion by at least 4.6 kcal mol^{-1} and requires overcoming energy barriers of 11.1 and 16.5 kcal mol^{-1}, respectively (Figure 6.A). The 1,2-insertion mode of isoprene at the terminal metal-allyl carbon bond has been also considered. It has been discarded as computed energy barriers are all above 26.5 kcal mol^{-1} (see SI, Table S3 and S4). Similar reactivity trends were computed for isoprene insertion into the *anti*-allyl system of complex ^{34C}**I•AlEt$_3$** (Figure 6.B). As for complex ^{34T}**I•AlEt$_3$**, insertion of *cis*-isoprene is kinetically more favorable than the one of *trans*-isoprene by at least 3 kcal mol^{-1}. Relative to the bimetallic complex ^{34C}**I•AlEt$_3$**, 1,4-insertion of *cis*-isoprene via transition state ^{14C}**I**^{34C}***Ip**** requires 13.7 kcal mol^{-1}.

Among, all insertion pathways, this one proceeds with the lowest energy barrier. The computed selectivity of at least 4.4 kcal mol^{-1} between *cis* / *trans* insertion is in fair agreement with the selectivity observed experimentally as a *cis* / *trans* ratio of 88 / 2 corresponds to $\Delta\Delta G^{\ddagger}$ of 2.2 kcal mol^{-1} at 20°C (Table 1, run 12). To a lesser extent, the difference of Gibbs energy barrier of 0.3 kcal mol^{-1} between insertion in the terminal allyl-Y carbon bond (linear chain growth) and in the central allyl-Y carbon bond (vinyl ramification) as shown in Figure 6.B, though in line with the selectivity observed experimentally, appears not large enough with respect to the $\Delta\Delta G^{\ddagger}$ value of 1.3 kcal mol^{-1} associated to a *cis-1,4 / 3,4 ratio of 88 / 10* at 20°C (Table 1, run 12). To test the influence of the counter-anion for this specific selectivity, transition state for *cis*-1,4-insertion and

cis-3,4-insertions have been optimized in presence of the counter-anion. In this case, the trend is maintained and the difference of Gibbs energy between the two transitions states is raised from 0.3 to 4.8 kcal.mol^{-1}. The difficulty in modeling both the counter-ion and the co-catalyst in - most likely - concerted mechanism defines a current limit of the state of the art of such computational mechanistic study.

CONCLUSION

The activation by alkylaluminum reagents of cationic complexes appears as an appealing alternative to the *in situ* generation of cationic polymerization catalyst since it provides better defined and structurally controlled species. This has been illustrated by the stereospecific polymerization of isoprene mediated by an Y-based mono-phenoxyimine cationic catalyst. In this case, the polymerization is living and *cis*-1,4 selective. Interestingly, it has been possible to switch the *cis* / *3,4* stereospecificity by replacing the phenoxy-imine ligand by an amidinate one. The associated computational mechanistic investigation performed at the DFT level has revealed the formation of Y/Al dormant heterobimetallic complexes and explained the absence of chain transfer between the Y active site and alkylaluminum counpound. Furthermore, based on the fair agreement between computed and experimental selectivities, we suggest that the active species is close to a bare cation that is protected / stabilized by alkylaluminum coupounds when not active.

EXPERIMENTAL SECTION

General procedure. All experiments were performed under a controlled atmosphere by using Schlenk and glovebox techniques for organometallic syntheses. THF and THF-d_8 was purified by distillation from sodium/benzophenone and degassed by freeze pump. Hexane, pentane, toluene and C_6D_6 were purified by distillation from NaK and degassed by freeze pump. Reagents: $[Y(CH_2SiMe_2Ph)_3(THF)_2]$,[34] $[Y(CH_2SiMe_2Ph)_3(THF)_4][B(C_6F_5)_4]$ (**3a'**),[35]

[$Y(CH_2C_6H_4NMe_2)_2(THF_2)][B(C_6F_5)_4$] (**3b'**),[35] [$L^1Y(CH_2SiMe_2Ph)_2(THF)$] (**1'**),[34] [PhC(N-2,6-$Pr^i_2C_6H_3)_2$]H (HL^2),[52] $Al(CH_2CMe_3)_3$[53] and $Al(CH_2SiMe_3)_3$[54] were prepared according to published procedures. $[PhNHMe_2][B(C_6F_5)_4]$ (Strem), TiBA, $HAl(^iBu)_2$, $Al(Oct)_3$ and Et_2AlCl (Aldrich) were used as received. Isoprene (Aldrich) was dried by stirring with CaH_2 for 48 hours and distilled under reduced pressure before use.

Characterization techniques.

Elemental analysis. Elemental analyses of the products were performed at the Mikroanalytisches Labor Pascher, Remagen (Germany).

Nuclear Magnetic Resonance analysis. NMR spectra were recorded on Bruker Advance III HD 400 MHz spectrometers in NMR tubes equipped with Teflon (Young) valve. ^1H NMR spectra were referenced to resonances of residual protons of deuterated solvents. ^{13}C NMR spectra were referenced to carbon resonances of deuterated solvents and reported in ppm relative to TMS. ^{89}Y NMR were externally referenced to 2 M YCl_3 in D_2O. INEPT experiment example: spectra were acquired at 24.51 MHz with a 5 s relaxation delay, with accumulation times of about 30 min (256 scans). HMBC experiment example: spectra were acquired at 24.51 MHz with pulse prog: hmbcgpndqf. A total of 256 t_1 increments were collected. Two transients were averaged for each increment and the recycling delay was 1.5 s. The experiment was optimized for $^2J_{H,Y} = 2.5$ Hz. Overall experiment time was 15 min. ^1H-coupled ^{89}Y INEPT experiment example: spectra were acquired at 24.51 MHz with a 5 s relaxation delay, with accumulation times of about 1 h (512 number of scan).

Size Exclusion Chromatography (SEC) analysis. Analyses were performed using a Viscotek system (from Malvern Instruments) equipped with pre-column (PLgel Olexis Guard 7.5x50mm) then three columns (PLgel Olexis Guard 7.5x300mm i.e. from Agilent Technologies). Detector

are composed of a refractometer, RALS (Right-Angle Light Scattering), LALS 7° (Low Angle Light Scattering) and viscometer. Portions (100 μL) of sample solutions with concentrations of 3 mg mL^{-1} were eluted in THF using a flow rate of 1 mL min^{-1} at 35 °C. The mobile phase was stabilized with 2,6-di-tert-butyl-4-methylphenol (200 mg L^{-1}). The OmniSEC software was used for data acquisition and data analysis. The molar masses were calculated with a light scattering detector.

MALDI-TOF mass spectrometry. Mass spectrometry was performed using a Voyager-DE Pro MALDI-TOF mass spectrometer (Sciex) equipped with nitrogen UV laser (λ=337 nm, 3 ns pulse). The sample was first diluted in 500μl of chloroform, then mixed with Dithranol (10g/l, chloroform) in a ratio 1/10 (sample/matrix, v/v). 1μl was deposed on the MALDI target and let dry at room temperature. The instrument was operated in the positive-reflectron mode (mass accuracy: 0.008%) with an accelerating potential of 20 kV. Typically, mass spectra were obtained by accumulation of 1200 laser shots for each analysis and processed using Data Explorer 4.0 software (Sciex).

Synthesis of $[L^1Y(CH_2SiMe_2Ph)(THF)_3][B(C_6F_5)_4]$ ***(1')***. A solution of $[PhNHMe_2][B(C_6F_5)_4]$ (202 mg, 0.25 mmol) in 7.5 mL of THF was added to a solution of $[L^1Y(CH_2SiMe_2Ph)_2(THF)]$ (200 mg, 0.25 mmol) in 7.5mL of THF. The reaction mixture was stirred at room temperature for 30 min. Part of THF was evaporated (¾ of the volume) and 10 mL of pentane were added. The suspension was cooled for 1 h at -30°C and two phases appeared, the upper phase was discarded, and 10 mL of pentane was added. The mixture was cooled for 1 h at -30°C, the solvent was discarded, and the yellow solid/oil was dried under vacuum to give **1'** (250 mg, 0.17 mmol, 68% yield). ^{1}H NMR (400 MHz, THF-d_8, 298K): δ = 8.48 (d, J_{HY} = 2 Hz, 1H, H-C=N), 7.65 (dd, J_{HH} = 8 Hz & 1.5 Hz, 1H, H-Ar), 7.6-7.0 (br, 9H, H-Ar), 6.87 (t, J_{HH} = 8 Hz, 1H, H-Ar), 3.65 (m, 12H,

THF), 2.89 (br, $CHMe_2$, 2H), 1.80 (m, 12H,THF), 1.55 (s, 9H, CMe_3), 1.33 (d, J_{HH} = 6.5 Hz, 6H, $CHMe_2$), 1.08 (d, J_{HH} = 6.5 Hz, 6H, $CHMe_2$), 0.10 (s, 6H, $SiMe_2$), -0.67 (br, 2H, Y-CH_2). ^{13}C NMR (100 MHz, THF-d_8, 298K): δ = 176.8 (C=N), 163.8 (C-O), 149.4 (C, Ar), 147.0 (C, Ar), 145.2 (C, Ar), 140.6 (C, Ar), 139.4 (C, Ar), 138.7 (C, Ar), 137.4 (C, Ar), 136.1 (C, Ar), 134.9 (C, Ar), 134.7 (C, Ar), 133.1 (C, Ar), 127.4 (C, Ar), 127.2 (C, Ar), 127.0 (C, Ar), 124.3 (C, Ar), 123.2 (C, Ar), 117.9 (C, Ar), 34.9 (CMe_3), 29.4 ((CMe_3), 28.4 ($CHMe_2$), 26.7 ($CHMe_2$), 1.6 ($SiMe_2$). ^{19}F NMR (376 MHz, THF-d_8, 298K): δ = -132.7 (br, 2F), -165.0 (t, J = 20 Hz, 1F), -168.5 (t, J = 18 Hz, 2F). ^{11}B NMR (128 MHz, THF-d_8, 298K): δ = -16.6.^{89}Y NMR (19.6 MHz, THF-d_8, 333K): δ = 413.2. Elemental analysis. Calcd for $C_{68}H_{66}BF_{20}NO_4SiY$: C, 55.60; H, 4.59; N, 0.95; B, 0.74. Found: C, 53.70; H, 4.41; N, 0.74; B 0.65.

*Synthesis of [L^2Y(CH_2SiMe_2Ph)$_2$(THF)] (**2**).* A solution of Y(CH_2SiMe_2Ph)$_3$(THF)$_2$ (0.4 g, 0.59 mmol) in hexane (30 mL) was added to [PhC(N-2,6-$Pr^i_2C_6H_3$)$_2$]H (0.26 g, 0.59 mmol) at room temperature. The reaction mixture was stirred for 3 hours, after which the volume of the solution was reduced to 10 mL. Cooling to -30°C overnight gave a white crystalline product (0.254 g, 0.28 mmol, 48% yield). ^{1}H NMR (400 MHz , C_6D_6, 298K): δ = 7.74 (m, 4H, *H*-Ar), 7.25-7.09 (br, 8H, *H*-Ar), 7.00 (s, 6H, *H*-Ar), 6.62 (m, 3H, *H*-Ar), 3.61 (sept, J = 7 Hz, 4H, C*H*Me_2), 3.42 (m, 4H, THF), 1.34 (d, J = 7Hz, 12H, CH*Me*$_2$), 0.99 (d, J = 7Hz, 12H, CH*Me*$_2$), 0.91 (m, 4H, THF), 0.49 (s, 12H, Si*Me*), 0.06 (d, J_{HY} = 3Hz, YC*H*$_2$). ^{13}C NMR (100 MHz, C_6D_6, 298K): δ = 174.6 (*C*=N), 145.8 (C, Ar), 142.9 (C, Ar), 141.9 (C, Ar), 142.0 (C, Ar), 133.5 (C, Ar), 130.2 (C, Ar), 129.0 (C, Ar), 126.8 (C, Ar), 124.5 (C, Ar), 123.7 (C, Ar), 70.1 (THF), 36.1 (d, J_{YC} = 40Hz, Y*C*H_2), 28.4 (*C*HMe_2), 25.5 (CH*Me*$_2$), 24.4 (THF), 23.2 (CH*Me*$_2$), 2.8 (Si*Me*$_2$). ^{89}Y NMR (19.6 MHz, C_6D_6, 298K): δ = 968.9. Calcd for $C_{53}H_{73}N_2OSi_2Y$: C, 70.79; H, 8.18; N, 3.12; Y, 9.89. Found: C, 69.71; H, 8.16; N, 3.17; Y 9.73.

*Synthesis of [L²Y(CH₂SiMe₂Ph)(THF)₃][B(C₆F₅)₄] (**2'**).* A solution of [PhNHMe₂][B(C₆F₅)₄] (178 mg, 0.22 mmol) in 4 mL of THF was added to a solution of [L²Y(CH₂SiMe₂Ph)₂(THF)] (200 mg, 0.22 mmol) in 4 mL of THF. The reaction mixture was stirred at room temperature for 30 min. Part of THF was evaporated (¾ of the volume) and 10 ml of pentane were added. The suspension was cooled for 1h at -30°C and two phases appeared, the upper phase was discarded, and 10 mL of pentane was added. The mixture was cooled for 1h at -30°C, the solvent was discarded, and the yellow solid/oil was dried under vacuum to give **2'** (200 mg, 0.12mmol, 56% yield).

^{1}H NMR (400 MHz , THF-d$_8$, 298K): δ = 7.60 (m, 3H, *H*-Ar), 7.32 (m, 4H, *H*-Ar), 7.11 (s, 6H, *H*-Ar), 6.97 (m, 3H, *H*-Ar), 3.65 (m, 12 H, THF), 3.35 (sept, J= 7 Hz, 4H, C*H*Me$_2$), 1.80 (m, THF), 1.26 ppm (d, J_{HH} = 7 Hz, 12H, CH*Me*$_2$), 0.89 ppm (d, J_{HH} = 7 Hz, 12H, CH*Me*$_2$), 0.28 (s, 6H, Si*Me*), 0.07 (d, J_{HY} = 3Hz, 2H, Y-C*H*$_2$).^{13}C NMR (100 MHz, THF-d$_8$, 298K): δ = 177.7 (*C*=N), 144.6 ppm (C Ar), 142.5 (*C* Ar), 141.6 (*C* Ar), 133.1 (*C* Ar), 133.0 (*C* Ar), 128.1 (*C* Ar), 127.4 (*C* Ar), 126.8 (*C* Ar), 125.3 (*C* Ar), 124.2 (*C* Ar), 38.3 (d, J_{YC} = 43 Hz, Y*C*H$_2$), 28.2 (*C*HMe$_2$), 25.4 (CH*Me*$_2$), 22.9 (CH*Me*$_2$), 1.9 (Si*Me*$_2$).^{19}F NMR (376 MHz, THF-d$_8$, 298K): δ = -132.7 (br, 2F), -165.0 (t, J = 20 Hz, 1F), -168.5 (t, J = 18 Hz, 2F). ^{11}B NMR (128 MHz, THF-d$_8$, 298K): δ = -16.6 ppm. ^{89}Y NMR (19.6 MHz, THF-d$_8$, 298K): δ = 525.9. Elemental analysis. Calcd for $C_{76}H_{76}BF_{20}N_2O_3SiY$: C, 58.02; H, 4.87; N, 1.78; Y, 5.65. Found: C, 57.39; H, 4.88; N, 1.79; Y, 5.67.

Typical procedure of isoprene polymerization.

Cationic precursor (representative example). In a glovebox, 2 mL of a 50 mM TiBA solution was diluted in 38 mL of toluene, then 2g (30 mmol) of isoprene were added. The solution was stirred overnight. This solution was added to a Schlenk tube containing 15 mg (0.01 mmol) of the cationic complex [L¹Y(CH₂SiMe₂Ph)(THF)₃][B(C₆F₅)₄] (**1'**). The mixture was stirred at 30 °C for one hour. After the designated time, the reaction was terminated by adding methanol, and the

polymer was precipitated and collected in a large amount of methanol. The polymer was then dried under dynamic vacuum at 70 °C for 3 hours.

Neutral precursor (representative example). In a glovebox, 2 mL of 50 mM TiBA solution was added in 33 mL of toluene, then 2g (30 mmol) of isoprene were added. The solution was stirred overnight. This solution was transferred to a Schlenk tube containing 8 mg (0.01 mmol) of $L^1Y(CH_2SiMe_2Ph)_2(THF)$ (**1**). A solution of 5 mL of toluene is prepared containing 9 mg (0.01 mmol) of trityl borate salt $[CPh_3][B(C_6F_5)_4]$. This solution is poured onto the solution containing the yttrium complex. The mixture was stirred at 30 °C for one hour. After the designated time, the reaction was terminated by adding methanol, and the polymer was precipitated and collected in a large amount of methanol. The polymer was then dried under dynamic vacuum at 70 °C for 3 hours.

Preparation of low molar mass polyisoprenes for chain-end analysis. 2 mL of TiBA solution (50 mM) was added in 3 mL of toluene, then 40 μl (0.4 mmol) of isoprene were added. The solution was stirred overnight. This solution was added to a Schlenk tube containing 16.5 mg (0.01 mmol) of $[L^1Y(CH_2SiMe_2Ph)(THF)_3][B(C_6F_5)_4]$ (**1'**). The mixture was stirred at room temperature for one hour. After the designated time, the reaction was terminated by adding dry methanol. The polymer was then dried under dynamic vacuum and then keep under argon.

Determination of the aluminum transfer efficiency. M_n calculation is based on the hypothesis of the formation of one chain per aluminum. Hence, % chain transfer efficiency $=100*m_{PI}/(M_n*n(AlR_3))$ in which m_{PI} = mass of isolated polyisoprene and $n(AlR_3)$ = number of mole of AlR_3 introduced.

Structure and reactivity. All calculations were performed using the Gaussian 09 D.01 suite of programs.[55] Electronic structure calculations were performed at the DFT level using the

B3PW91[44,45] functional. The Stuttgart-Cologne small-core quasi-relativistic pseudopotential ECP28MWB[56] and its available basis set including up to the g function was used to describe yttrium.[57] Similarly, silicon and phosphorus were represented by a Stuttgart−Dresden−Bonn pseudopotential[58] along with the related basis set augmented by a *d* function of polarization (α_d(P) = 0.387; α_d(Si) = 0.284). Other atoms were described by a polarized all electron triple-ζ 6-311G(*d*,*p*) basis set.[59] Bulk solvent effect of toluene or THF were simulated using the SMD continuum model.[48] The Grimme empirical correction with the original D3 damping function was used to include the dispersion correction as a single point calculation.[46,47] Transition state optimization was followed by frequency calculations to characterize the stationary point. Intrinsic reaction coordinate (IRC) calculations were performed to confirm the connectivity of the transition states. Gibbs energies were estimated within the harmonic oscillator approximation, and estimated at 298 K and 1 atm.

ASSOCIATED CONTENT

Supporting Information. NMR spectra, MALDI-TOF mass spectrometry, energy profiles and additional structural sampling are provided as a supplementary material, as well as all the Cartesian coordinates, associated computed energies. The following files are available free of charge.

AUTHOR INFORMATION

Corresponding Authors

* e-mail for C.B.: mostafa.taoufik@univ-lyon1.fr

* e-mail for M.T.: christophe.boisson@univ-lyon1.fr

* e-mail for L.P.: lionel.perrin@univ-lyon1.fr

Author Contributions

The manuscript was written through contributions of all authors. All authors have given approval to the final version of the manuscript.

Funding Sources

The authors thank IFP Energies nouvelles and Michelin for financial support. L.P thanks the CNRS and le Ministère de l'Enseignement Supérieur et de la Recherche (MESR) for funding.

Notes

The authors declare no competing financial interest.

ACKNOWLEDGMENT

L.V. and L.P. thank CCIR facility of ICBMS and P2CHPD computer center of Université Lyon 1 for generous donations of computational time and technical support. L.P. thanks CCIR facility of ICBMS and P2CHPD computer center of Université Lyon 1 for generous donations of computational time and technical support. The authors thank the Centre Commun de RMN at ICBMS for NMR analyses and Emmanuel Chefdeville for assistance for INEPT experiments.

REFERENCES

(1) Ricci, G.; Pampaloni, G.; Sommazzi, A.; Masi, F. Dienes Polymerization: Where We Are and What Lies Ahead. *Macromolecules* **2021**, *54*, 5879-5914.

(2) Kaminsky, W.; Arndt, M.; Bhm, L. L.; Vogt, D.; Chauvin, Y.; Olivier, H.; Henkelmann, J.; Taube, R.; Sylvester, G.; Mol, J. C.; Drent, E.; van Broekhoven, J. A. M.; Budzelaar, P. H. M.;

Yoshimura, N.; Wilke, G.; Eckerle, A. Reactions of Unsaturated Compounds. In *Applied Homogeneous Catalysis with Organometallic Compounds*, 1996; pp 220-273.

(3) Zeimentz, P. M.; Arndt, S.; Elvidge, B. R.; Okuda, J. Cationic organometallic complexes of scandium, yttrium, and the lanthanoids. *Chem Rev* **2006**, *106*, 2404-2433.

(4) Zhang, Z.; Cui, D.; Wang, B.; Liu, B.; Yang, Y. Polymerization of 1,3-Conjugated Dienes with Rare-Earth Metal Precursors. In *Molecular Catalysis of Rare-Earth Elements*, Roesky, P. W. Ed.; Springer Berlin Heidelberg, 2010; pp 49-108.

(5) Yang, F. Z.; Li, X. F. Novel Cationic Rare Earth Metal Alkyl Catalysts for Precise Olefin Polymerization. *J. Polym. Sci. A: Polym. Chem.* **2017**, *55*, 2271-2280.

(6) Hou, Z. M.; Wakatsuki, Y. Recent developments in organolanthanide polymerization catalysts. *Coord. Chem. Rev.* **2002**, *231*, 1-22.

(7) Fischbach, A.; Anwander, R. Rare-Earth Metals and Aluminum Getting Close in Ziegler-Type Organometallics. In *Neodymium Based Ziegler Catalysts – Fundamental Chemistry*, Nuyken, O. Ed.; Springer Berlin Heidelberg, 2006; pp 155-281.

(8) Friebe, L.; Nuyken, O.; Obrecht, W. Neodymium-Based Ziegler/Natta Catalysts and their Application in Diene Polymerization. In *Neodymium Based Ziegler Catalysts – Fundamental Chemistry*, Nuyken, O. Ed.; Springer Berlin Heidelberg, 2006; pp 1-154.

(9) Arndt, S.; Beckerle, K.; Zeimentz, P. M.; Spaniol, T. P.; Okuda, J. Cationic yttrium methyl complexes as functional models for polymerization catalysts of 1,3-dienes. *Angew. Chem. Int. Ed.* **2005**, *44*, 7473-7477.

(10) Robert, D.; Abinet, E.; Spaniol, T. P.; Okuda, J. Cationic allyl complexes of the rare-earth metals: synthesis, structural characterization, and 1,3-butadiene polymerization catalysis. *Chem. Eur. J* **2009**, *15*, 11937-11947.

(11) Maiwald, S.; Weißenborn, H.; Windisch, H.; Sommer, C.; Müller, G.; Taube, R. Zur Katalyse der stereospezifischen Butadienpolymerisation. *Macromol. Chem. Phys.* **1997**, *198*, 3305-3315.

(12) Ajellal, N.; Furlan, L.; Thomas, C. M.; Casagrande, O. L.; Carpentier, J. F. Mixed aluminum-magnesium-rare earth allyl catalysts for controlled isoprene polymerization: Modulation of stereocontrol. *Macromol. Rapid Commun.* **2006**, *27*, 338-343.

(13) Maiwald, S.; Sommer, C.; Müller, G.; Taube, R. On the 1,4-cis-Polymerization of Butadiene with the Highly Active Catalyst Systems $Nd(C_3H_5)_2Cl$ 1.5THF/Hexaisobutylaluminoxane (HIBAO), $Nd(C_3H_5)Cl_2$ 2THF/HIBAO and $Nd(C_3H_5)Cl_2$ 2THF/Methyl-aluminoxane (MAO) – Degree of Polymerization, Polydispersity, Kinetics and Catalyst Formation. *Macromol. Chem. Phys.* **2001**, *202*, 1446-1456.

(14) Maiwald, S.; Sommer, C.; Müller, G.; Taube, R. Highly Active Single-Site Catalysts for the 1,4-cis Polymerization of Butadiene from Allylneodymium(III) Chlorides and Trialkylaluminiums – A Contribution to the Activation of Tris(allyl)neodymium(III) and the Further Elucidation of the Structure-Activity Relationship. *Macromol. Chem. Phys.* **2002**, *203*, 1029-1039.

(15) Zimmermann, M.; Tornroos, K. W.; Anwander, R. Cationic rare-earth-metal half-sandwich complexes for the living trans-1,4-isoprene polymerization. *Angew. Chem. Int. Ed.* **2008**, *47*, 775-778.

(16) Liu, H.; He, J. Y.; Liu, Z. X.; Lin, Z. G.; Du, G. X.; Zhang, S. W.; Li, X. F. Quasi-Living trans-1,4-Polymerization of Isoprene by Cationic Rare Earth Metal Alkyl Species Bearing a Chiral (S,S)-Bis(oxazolinylphenyl)amido Ligand. *Macromolecules* **2013**, *46*, 3257-3265.

(17) Zhang, L.; Luo, Y.; Hou, Z. Unprecedented isospecific 3,4-polymerization of isoprene by cationic rare earth metal alkyl species resulting from a binuclear precursor. *J. Am. Chem. Soc.* **2005**, *127*, 14562-14563.

(18) Zhang, L.; Nishiura, M.; Yuki, M.; Luo, Y.; Hou, Z. Isoprene polymerization with yttrium amidinate catalysts: switching the regio- and stereoselectivity by addition of $AlMe_3$. *Angew. Chem. Int. Ed.* **2008**, *47*, 2642-2645.

(19) Li, S. H.; Cui, D. M.; Li, D. F.; Hou, Z. M. Highly 3,4-Selective Polymerization of Isoprene with NPN Ligand Stabilized Rare-Earth Metal Bis(alkyl)s. Structures and Performances. *Organometallics* **2009**, *28*, 4814-4822.

(20) Wang, B.; Cui, D.; Lv, K. Highly 3,4-Selective Living Polymerization of Isoprene with Rare Earth Metal Fluorenyl N-Heterocyclic Carbene Precursors. *Macromolecules* **2008**, *41*, 1983-1988.

(21) Zhang, L.; Suzuki, T.; Luo, Y.; Nishiura, M.; Hou, Z. Cationic alkyl rare-earth metal complexes bearing an ancillary bis(phosphinophenyl)amido ligand: a catalytic system for living cis-1,4-polymerization and copolymerization of isoprene and butadiene. *Angew. Chem. Int. Ed.* **2007**, *46*, 1909-1913.

(22) Gao, W.; Cui, D. Highly cis-1,4 selective polymerization of dienes with homogeneous Ziegler-Natta catalysts based on NCN-pincer rare earth metal dichloride precursors. *J. Am. Chem. Soc.* **2008**, *130*, 4984-4991.

(23) Li, X.; Nishiura, M.; Hu, L.; Mori, K.; Hou, Z. Alternating and random copolymerization of isoprene and ethylene catalyzed by cationic half-sandwich scandium alkyls. *J. Am. Chem. Soc.* **2009**, *131*, 13870-13882.

(24) Bonnet, F.; Da Costa Violante, C.; Roussel, P.; Mortreux, A.; Visseaux, M. Unprecedented dual behaviour of a half-sandwich scandium-based initiator for both highly selective isoprene and styrene polymerisation. *Chem. Commun.* **2009**, 3380-3382.

(25) Yang, Y.; Wang, Q. Y.; Cui, D. M. Isoprene polymerization with indolide-imine supported rare-earth metal alkyl and amidinate complexes. *J. Polym. Sci. A: Polym. Chem.* **2008**, *46*, 5251-5262.

(26) Zhang, P. F.; Liao, H. Y.; Wang, H. H.; Li, X. F.; Yang, F. Z.; Zhang, S. W. Cis-1,4-Polymerization of Isoprene Catalyzed by 1,3-Bis(2-pyridylimino)isoindoline-Ligated Rare-Earth-Metal Dialkyl Complexes. *Organometallics* **2017**, *36*, 2446-2451.

(27) Lv, K.; Cui, D. M. CCC-Pincer Bis(carbene) Lanthanide Dibromides. Catalysis on Highly cis-1,4-Selective Polymerization of Isoprene and Active Species. *Organometallics* **2010**, *29*, 2987-2993.

(28) Pan, Y.; Xu, T.; Yang, G. W.; Jin, K.; Lu, X. B. Bis(oxazolinyl)phenyl-ligated rare-earth-metal complexes: highly regioselective catalysts for cis-1,4-polymerization of isoprene. *Inorg. Chem.* **2013**, *52*, 2802-2808.

(29) Döring, C.; Kretschmer, W. P.; Bauer, T.; Kempe, R. Scandium Aminopyridinates: Synthesis, Structure and Isoprene Polymerization. *Eur. J. Inorg. Chem.* **2009**, *2009*, 4255-4264.

(30) Yu, N.; Nishiura, M.; Li, X.; Xi, Z.; Hou, Z. Cationic scandium allyl complexes bearing mono(cyclopentadienyl) ligands: synthesis, novel structural variety, and olefin-polymerization catalysis. *Chem. Asian. J.* **2008**, *3*, 1406-1414.

(31) Makio, H.; Fujita, T. Development and application of FI catalysts for olefin polymerization: unique catalysis and distinctive polymer formation. *Acc. Chem. Res.* **2009**, *42*, 1532-1544.

(32) Wang, C.; Friedrich, S.; Younkin, T. R.; Li, R. T.; Grubbs, R. H.; Bansleben, D. A.; Day, M. W. Neutral Nickel(II)-Based Catalysts for Ethylene Polymerization. *Organometallics* **1998**, *17*, 3149-3151.

(33) Suzuki, Y.; Kinoshita, S.; Shibahara, A.; Ishii, S.; Kawamura, K.; Inoue, Y.; Fujita, T. Trimerization of Ethylene to 1-Hexene with Titanium Complexes Bearing Phenoxy-Imine Ligands with Pendant Donors Combined with MAO. *Organometallics* **2010**, *29*, 2394-2396.

(34) Emslie, D. J. H.; Piers, W. E.; Parvez, M.; McDonald, R. Organometallic Complexes of Scandium and Yttrium Supported by a Bulky Salicylaldimine Ligand. *Organometallics* **2002**, *21*, 4226-4240.

(35) Oswald, A. D.; El Bouhali, A.; Chefdeville, E.; Breuil, P. A. R.; Olivier-Bourbigou, H.; Thuilliez, J.; Vaultier, F.; De Mallmann, A.; Taoufik, M.; Perrin, L.; Boisson, C. Monocationic Bis-Alkyl and Bis-Allyl Yttrium Complexes: Synthesis, Y- 89 NMR Characterization, Ethylene or Isoprene Polymerization, and Modeling. *Organometallics* **2021**, *40*, 218-230.

(36) Bambirra, S.; Bouwkamp, M. W.; Meetsma, A.; Hessen, B. One ligand fits all: cationic mono(amidinate) alkyl catalysts over the full size range of the group 3 and lanthanide metals. *J. Am. Chem. Soc.* **2004**, *126*, 9182-9183.

(37) Bambirra, S.; van Leusen, D.; Meetsma, A.; Hessen, B.; Teuben, J. H. Yttrium alkyl complexes with a sterically demanding benzamidinate ligand: synthesis, structure and catalytic ethene polymerisation. *Chem. Commun.* **2003**, 522-523.

(38) Yu, X.; You, Q.; Zhou, X.; Zhang, L. Isoprene Regioblock Copolymerization: Switching the Regioselectivity by the in Situ Ancillary Ligand Transmetalation of Active Yttrium Species. *ACS Catal.* **2018**, *8*, 4465-4472.

(39) Valente, A.; Mortreux, A.; Visseaux, M.; Zinck, P. Coordinative chain transfer polymerization. *Chem. Rev.* **2013**, *113*, 3836-3857.

(40) Rodrigues, A. S.; Kirillov, E.; Vuillemin, B.; Razavi, A.; Carpentier, J. F. Binary ansa-lanthanidocenes/dialkylmagnesium systems versus single-component catalyst: Controlled synthesis of end-capped syndiotactic oligostyrenes. *J. Mol. Catal. A Chem.* **2007**, *273*, 87-91.

(41) Liu, B.; Cui, D. M. Regioselective Chain Shuttling Polymerization of Isoprene: An Approach To Access New Materials from Single Monomer. *Macromolecules* **2016**, *49*, 6226-6231.

(42) Jian, Z.; Cui, D.; Hou, Z.; Li, X. Living catalyzed-chain-growth polymerization and block copolymerization of isoprene by rare-earth metal allyl precursors bearing a constrained-geometry-conformation ligand. *Chem. Commun.* **2010**, *46*, 3022-3024.

(43) Verrieux, L.; Thuilliez, J.; Jean-Baptiste-dit-Dominique, F.; Boisson, C.; Poradowski, M.-N.; Perrin, L. Ene/Diene Copolymerization Catalyzed by Cationic Sc and Gd d0 Metal Complexes: Speciation, Ion Pairing, and Selectivity from a Computational Perspective. *ACS Catal.* **2020**, *10*, 12359-12369.

(44) Becke, A. D. Density-Functional Thermochemistry .3. The Role of Exact Exchange. *J. Chem. Phys.* **1993**, *98*, 5648-5652.

(45) Perdew, J. P.; Wang, Y. Accurate and simple analytic representation of the electron-gas correlation energy. *Phys Rev B Condens Matter* **1992**, *45*, 13244-13249.

(46) Grimme, S.; Antony, J.; Ehrlich, S.; Krieg, H. A consistent and accurate ab initio parametrization of density functional dispersion correction (DFT-D) for the 94 elements H-Pu. *J. Chem. Phys.* **2010**, *132*, 154104.

(47) Grimme, S.; Ehrlich, S.; Goerigk, L. Effect of the damping function in dispersion corrected density functional theory. *J. Comput. Chem.* **2011**, *32*, 1456-1465.

(48) Marenich, A. V.; Cramer, C. J.; Truhlar, D. G. Universal solvation model based on solute electron density and on a continuum model of the solvent defined by the bulk dielectric constant and atomic surface tensions. *J. Phys. Chem. B* **2009**, *113*, 6378-6396.

(49) Belaid, I.; Macqueron, B.; Poradowski, M. N.; Bouaouli, S.; Thuilliez, J.; Da Cruz-Boisson, F.; Monteil, V.; D'Agosto, F.; Perrin, L.; Boisson, C. Identification of a Transient but Key Motif in the Living Coordinative Chain Transfer Cyclocopolymerization of Ethylene with Butadiene. *ACS Catal.* **2019**, *9*, 9298-9309.

(50) Nsiri, H.; Belaid, I.; Larini, P.; Thuilliez, J.; Boisson, C.; Perrin, L. Ethylene-Butadiene Copolymerization by Neodymocene Complexes: A Ligand Structure/Activity/Polymer Microstructure Relationship Based on DFT Calculations. *ACS Catal.* **2016**, *6*, 1028-1036.

(51) Belaid, I.; Poradowski, M. N.; Bouaouli, S.; Thuilliez, J.; Perrin, L.; D'Agosto, F.; Boisson, C. Dialkenylmagnesium Compounds in Coordinative Chain Transfer Polymerization of Ethylene. Reversible Chain Transfer Agents and Tools To Probe Catalyst Selectivities toward Ring Formation. *Organometallics* **2018**, *37*, 1546-1554.

(52) Nijhuis, C. A.; Jellema, E.; Sciarone, T. J. J.; Meetsma, A.; Budzelaar, P. H. M.; Hessen, B. First-Row Transition Metal Bis(amidinate) Complexes; Planar Four-Coordination of Fe(II) Enforced by Sterically Demanding Aryl Substituents. *Eur. J. Inorg. Chem.* **2005**, *2005*, 2089-2099.

(53) Beachley, O. T.; Pazik, J. C. Synthesis and characterization of neopentylgallium compounds. *Organometallics* **2002**, *7*, 1516-1519.

(54) Kramer, M. U.; Robert, D.; Nakajima, Y.; Englert, U.; Spaniol, T. P.; Okuda, J. Alkyl Abstraction from a Trialkylyttrium Complex [$YR_3(thf)_2$] (R = CH_2SiMe_3) Using a Group13 Element Lewis Acid ER_3 (E = B, Al, Ga, In) – Structural Characterisation of the Ion Pair $[YR_2(thf)_4]^+[GaR_4]^-$ and of ER_3 (E = B, Al, Ga). *Eur. J. Inorg. Chem.* **2007**, *2007*, 665-674.

(55) Gaussian 09, Revision D.01, Frisch, M. J.; Trucks, G. W.; Schlegel, H. B.; Scuseria, G. E.; Robb, M. A.; Cheeseman, J. R.; Scalmani, G.; Barone, V.; Mennucci, B.; Petersson, G. A.; Nakatsuji, H.; Caricato, M.; Li, X.; Hratchian, H. P.; Izmaylov, A. F.; Bloino, J.; Zheng, G.; Sonnenberg, J. L.; Hada, M.; Ehara, M.; Toyota, K.; Fukuda, R.; Hasegawa, J.; Ishida, M.; Nakajima, T.; Honda, Y.; Kitao, O.; Nakai, H.; Vreven, T.; Montgomery Jr., J. A.; Peralta, J. E.; Ogliaro, F.; Bearpark, M.; Heyd, J. J.; Brothers, E.; Kudin, K. N.; Staroverov, V. N.; Kobayashi, R.; Normand, J.; Raghavachari, K.; Rendell, A.; Burant, J. C.; Iyengar, S. S.; Tomasi, J.; Cossi, M.; Rega, N.; Millam, J. M.; Klene, M.; Knox, J. E.; Cross, J. B.; Bakken, V.; Adamo, C.; Jaramillo, J.; Gomperts, R.; Stratmann, R. E.; Yazyev, O.; Austin, A. J.; Cammi, R.; Pomelli, C.; Ochterski, J. W.; Martin, R. L.; Morokuma, K.; Zakrzewski, V. G.; Voth, G. A.;. Salvador, P; Dannenberg, J. J.; Dapprich, S.; Daniels, A. D.; Farkas, Ö.; Foresman, J. B.; Ortiz, J. V.; Cioslowski, J.; Fox, D. J. Gaussian, Inc., Wallingford CT, 2009.

(56) Andrae, D.; Häußermann, U.; Dolg, M.; Stoll, H.; Preuß, H. Energy-adjustedab initio pseudopotentials for the second and third row transition elements. *Theor. Chim. Acta* **1990**, *77*, 123-141.

(57) Martin, J. M. L.; Sundermann, A. Correlation consistent valence basis sets for use with the Stuttgart-Dresden-Bonn relativistic effective core potentials: The atoms Ga-Kr and In-Xe. *J. Chem. Phys.* **2001**, *114*, 3408-3420.

(58) Bergner, A.; Dolg, M.; Kuchle, W.; Stoll, H.; Preuß, H. Ab-Initio Energy-Adjusted Pseudopotentials for Elements of Groups 13-17. *Mol. Phys.* **1993**, *80*, 1431-1441.

(59) McLean, A. D.; Chandler, G. S. Contracted Gaussian basis sets for molecular calculations. I. Second row atoms, Z=11–18. *J. Chem. Phys.* **1980**, *72*, 5639-5648.

GRAPHICAL TOC